Journal of Molecular Structure 1081 (2015) 536–542

Contents lists available at ScienceDirect

Journal of Molecular Structure

journal homepage: www.elsevier.com/locate/molstruc

Theoretical study on the molecular structure and vibrational properties, NBO and HOMO–LUMO analysis of the POX_3 (X = F, Cl, Br, I) series of molecules

Jorge E. Galván [a,b], Diego M. Gil [a,b], Hernán E. Lanús [a], Aida Ben Altabef [a,b,*,1]

[a] Instituto de Química Física, Facultad de Bioquímica, Química y Farmacia, Universidad de Tucumán, San Lorenzo 456, T4000CAN S.M. de Tucumán, Argentina
[b] INQUINOA-CONICET, San Lorenzo 456, T4000CAN, San Miguel de Tucumán, Argentina

HIGHLIGHTS

- The fourth member of the compounds POX_3 with X = I was synthesized and characterized by infrared spectroscopy.
- The molecular structure of POX_3 (X = F, Cl, Br, I) molecules were investigated by means DFT and *ab-initio* methods.
- NBO analysis was performed in order to know the hyper-conjugative interactions that favor one structure over another.
- HOMO and LUMO analysis have been performed to know global descriptors and reactivity of the molecules.

GRAPHICAL ABSTRACT

Frontier molecular orbitals and HOMO–LUMO band gap for: (a) POF_3, (b) $POCl_3$, (c) $POBr_3$, (d) POI_3.

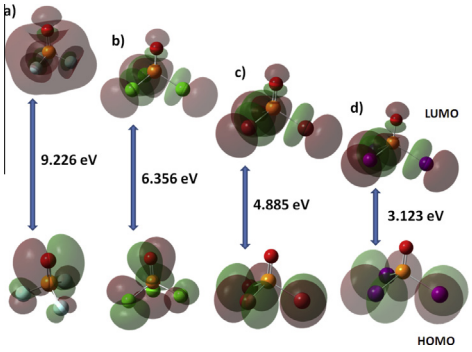

ARTICLE INFO

Article history:
Received 28 July 2014
Received in revised form 5 September 2014
Accepted 23 October 2014
Available online 6 November 2014

Keywords:
Infrared and Raman spectroscopy
Quantum chemical calculation
POX_3
NBO analysis
HOMO–LUMO

ABSTRACT

The fourth member of the series of compounds of the type POX_3 with X = I was synthesized and characterized by infrared spectroscopy. The geometrical parameters and vibrational properties of POX_3 (X = F, Cl, Br, I) molecules were investigated theoretically by means DFT and *ab initio* methods. Available geometrical and vibrational data were used together with theoretical calculations in order to obtain a set of scaled force constants. The observed trends in geometrical parameters are analyzed and compared with those obtained in a previous work for the VOX_3 (X = F, Cl, Br, I) series of compounds. NBO analysis was performed in order to know the hyper-conjugative interactions that favor one structure over another. The molecular properties such as ionization potential, electron affinity, electronegativity, chemical potential, chemical hardness, softness and global electrophilicity index have been deduced from HOMO–LUMO analysis.

Introduction

Chemistry of phosphorous halides is of special interest, if only because it is out of phosphorous halides that the overwhelming majority or rather almost all known at present phosphorous–organic compounds are obtained. The molecular structure and

* Corresponding author at: Instituto de Química Física, Facultad de Bioquímica, Química y Farmacia, Universidad Nacional de Tucumán, San Lorenzo 456, T4000CAN Tucumán. Argentina. Tel.: +54 381 4311044; fax: +54 381 4248169.
E-mail address: altabef@fbqf.unt.edu.ar (A.B. Altabef).
[1] Member of the Carrera del Investigador Científico, CONICET, Argentina

http://dx.doi.org/10.1016/j.molstruc.2014.10.060
0022-2860/

the geometrical parameters of $POCl_3$, POF_3 and $POBr_3$ were determined previously by gas electron diffraction (GED), and microwave spectroscopy [1–4]. Infrared and Raman spectra of these compounds in the solid, liquid and gaseous phase and in different noble gases matrices have been reported previously by different authors [5–11]. Recently, a new route of synthesis have been reported using $POCl_3$ as row material for the production of POX_3 (X = F, Br, I) [12]. In this reaction, the $POCl_3$ reacts with the metallic halide in solid state in a furnace at temperatures higher than 450 °C [12]. Sheldon et al. have reported the synthesis of addition compounds by using metal halides such as $AlCl_3$ with POX_3 compounds. The infrared spectroscopy was used to follow the synthesis of these compounds because the P—O stretching band shifts to lower frequency with respect to the pure phosphoryl halide indicating that the bonding in the addition compounds is through of the O atom [13].

Several authors have studied the molecular force fields of POF_3, $POCl_3$ and $POBr_3$ by approximate methods including Coriolis coupling constants and isotopic displacements [5,8,14–17], but none of them employed a quantum chemistry method as the one we report here.

In this paper, we report the calculations of geometrical parameters and vibrational spectra of the phosphorus oxotrihalides as well as other molecular properties at different levels of theory. Natural bond orbital (NBO) analysis was also performed in order to understand the possible hyper-conjugation interactions present in the different compounds of the series. HOMO–LUMO analysis was performed in order to elucidate information regarding ionization potential (*IP*), electron affinity (*EA*), electronegativity (χ), electrophilicity index (ω), hardness (η), softness (s) and chemical potential (μ). We also report the scaled molecular force fields for POF_3, $POCl_3$ and $POBr_3$. Moreover, we present a comparative analysis of the results obtained for these series with the ones derived for the VOX_3 (X = F, Cl, Br, I) molecules in a previous work [18].

Experimental

Synthesis

The compound POI_3 was synthesized according to Kostina et al. [19]. The reaction was performed using Methyl phosphorodiiodidites (CH_3POI_2) with iodine in CCl_4 as solvent. The compound CH_3POI_2 was first synthesized by mixing stoichiometric amounts of CH_3POCl_2 with LiI in CCl_4 [20]. In order to prevent the hydrolysis of the final product by atmospheric moisture, the synthesis was made in a dry box at −20 °C using an acetone bath with liquid N_2. POI_3 is a dark violet crystalline substance very soluble in CCl_4 and alkyl iodides. Only IR spectroscopy was used to characterize the compound because it is very unstable in air conditions.

FTIR spectroscopy

The room temperature (RT) infrared spectrum of POI_3 in solid state was recorded in KBr pellets in the 4000–400 cm^{-1} frequency range with a Perkin–Elmer GX1 Fourier Transform infrared instrument. The Raman spectrum of the substance has not been measured due to the low stability of the compound in air atmosphere.

Computational methods

Theoretical calculations were performed using the program package Gaussian 03 [21]. Geometry optimizations were performed at the MP2 [22] and DFT levels using a variety of basis sets. Electron correlation was then considered using the MP2 approach with the LanL2DZ, 6-31G(d), 6-311G(d,p) and 6-311++G(d,p) basis sets [23–26]. DFT calculations were performed using Becke's three-parameter hybrid exchange functional [27] (B3) combined with both the Lee–Yang–Parr gradient-corrected correlation functional [28] (LYP) and the same basis sets as for the MP2 calculations. The second DFT method used, mPW1PW91 [29] applies a modified Perdew–Wang exchange functional and Perdew–Wang 91 correlation functional [29]. These methods of calculation were used in order to reproduce better the experimental results reported by different experimental methods such as GED and microwave measurements. A very good correlation between experimental and theoretical geometrical parameters calculated by MP2 and DFT methods was obtained by different molecules studied in our group of work [30–32]. For POI_3 the calculations were performed using LanL2DZ basis sets for iodine atoms and other basis sets for the rest of atoms. All calculations were performed using standard gradient techniques and default convergence criteria. The stability of the optimized geometries was confirmed by wavenumber calculations, which gave positive values for all the obtained wavenumbers. The vibrational modes were assigned by means of visual inspection using the GaussView 05 program [33]. A comparison was performed between the theoretically calculated frequencies and the experimentally measured frequencies. In this investigation we observed that the calculated frequencies were slightly greater than the fundamental frequencies.

A natural bond orbital (NBO) calculation was performed at the B3LYP/6-311++G(d,p) level using the program NBO 3.1 [34] as implemented in Gaussian 03 package. This analysis were performed in order to understand various second order interactions between the filled orbitals of one subsystem and vacant orbitals of another subsystem, in order to have a measure of the intramolecular delocalization of hyper-conjugation.

The molecular properties such as ionization potential, electronegativity, chemical potential, chemical hardness and softness have been deduced from HOMO–LUMO analysis employing B3LYP method with different basis sets.

Theoretical force constants matrices in cartesian coordinates from Gaussian were transformed to symmetry coordinates through the corresponding B matrix on the FCARTP program [35]. The resulting force constants were scaled on the same program using the scheme of Pulay et al. [36], in which each diagonal force constant is multiplied by a scale factor $f_a f_b, \ldots$ and the off-diagonal force constants are multiplied by $(f_a f_b)^{1/2}$, in order to reproduce the experimental wavenumbers. Potential energy distributions were also obtained from the resulting scaled force field in order to confirm or reassign the earlier empirical assignments.

Results and discussion

Quantum chemical calculations

Molecular geometry and structural properties

Optimized geometrical parameters for POI_3 are presented in Table 1. The geometrical parameters calculated at different levels of theory for POF_3, $POCl_3$ and $POBr_3$ are shown in Tables S1–S3, respectively. A comparison between the calculated geometrical parameters with the experimental ones using different levels of theory and basis sets was carried out. The molecular structure of the series of compounds with general formula POX_3 are shown in Fig. 1. According to the values calculated at MP2/6-311++G(d,p) level, an increase in the P=O bond length is observed along the series. The P=O bond length calculated for POF_3 is 1.449 Å and the value calculated for POI_3 is 1.478 Å. For the case of POI_3, the high atomic volume of the halogen atom produces a lengthening of the P=O bond length according to the results reported in Table 1. This is in agreement with the experimental trend, except when

Table 1
Optimized geometrical parameters calculated with different methods and basis sets for POI_3 compound.

Method	Basis sets[a]	P═O	P—I	I—P—O	I—P—I
HF	6-31G(d)	1.448	2.465	112.8	105.9
	6-311G(d,p)	1.439	2.458	113.0	105.9
	6-311++G(d,p)	1.441	2.450	112.9	105.8
B3LYP	6-31G(d)	1.481	2.519	113.2	105.4
	6-311G(d,p)	1.473	2.518	113.3	105.3
	6-311++G(d,p)	1.475	2.508	113.2	105.5
MP2	6-31G(d)	1.491	2.496	113.1	105.6
	6-311G(d,p)	1.476	2.492	113.2	105.5
	6-311++G(d,p)	1.478	2.479	113.1	105.6
mPW1mPw91	6-31G(d)	1.476	2.482	113.3	105.4
	6-311G(d,p)	1.467	2.481	113.4	105.2
	6-311++G(d,p)	1.468	2.471	113.4	105.3

[a] The calculations were performed with LanL2DZ basis sets for the iodine atom and the other basis sets for P and O atoms. The RMSD values were not reported in this table because of experimental values were not informed previously.

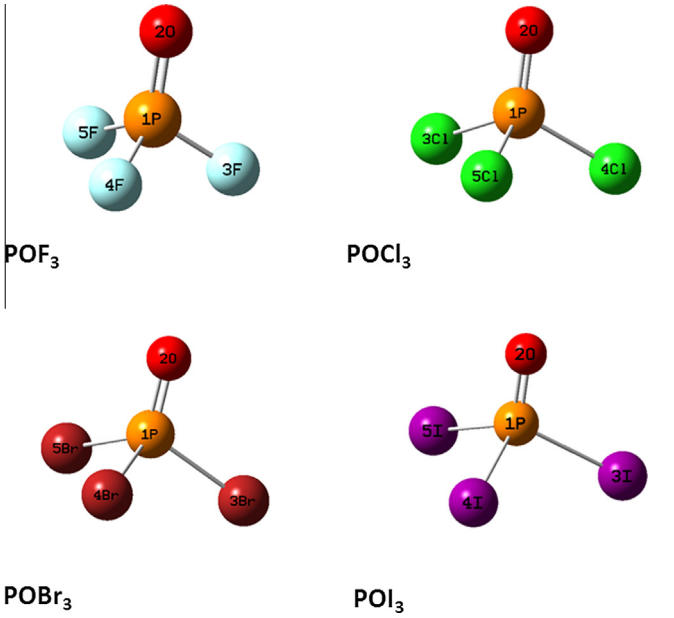

Fig. 1. Optimized molecular structure of the series of molecules with general formula POX_3 (X = F, Cl, Br, I).

going from the chlorine to the bromine compound, where the P═O bond length is shorter than expected. This trend goes together with a decrease in energy of the P—O bond, reflected in a lower frequency of vibration for the P═O stretching mode (see below). Considering the X—P—X bond angle, an increase was observed along the series. For POF_3, the angle calculated is 100.6° and the value reported for POI_3 is 105.6°. Similar results were reported for the series of compounds VOX_3 (X = F, Cl, Br and I) [18]. Opposite results were observed for the X—P—O bond angles.

NBO analysis

Natural bond orbital (NBO) analysis is a useful tool for understanding delocalization of electron density from occupied Lewis-type (donor) NBOs to properly unoccupied non-Lewis type (acceptor) NBOs within the molecule. The stabilization of orbital interaction is proportional to the difference energy between the interacting orbitals. Therefore, the interaction having strongest stabilization takes place between effective donors and effective acceptors. The interaction between bonding and anti-bonding molecular orbitals can be quantitatively described in terms of NBO approach that is expressed by means of second-order

Table 2
Second-order perturbation theory analysis of the Fock matrix for POX_3 compounds (X = F, Cl, Br, I) by the NBO method.

Interaction (donor → acceptor)[a]	$E(2)$ in kcal mol^{-1}[b]			
	POF_3	$POCl_3$	$POBr_3$	POI_3
LP O(2) → σ* P(1)—X(3)	0.67	37.16	38.44	36.26
LP O(2) → σ* P(1)—X(4)	0.67	38.16	38.44	36.26
LP O(2) → σ* P(1)—X(5)	0.67	38.17	38.44	36.26
LP X(3) → σ* P(1)—O(2)	37.26	4.57	3.48	2.93
LP X(3) → σ* P(1)—X(3)	0.64	–	–	–
LP X(3) → σ* P(1)—X(4)	5.90	6.77	5.04	3.49
LP X(3) →σ* P(1)—X(5)	5.91	6.77	5.04	3.49
LP X(4) → σ* P(1)—O(2	36.84	4.57	3.48	2.93
LP X(4) → σ* P(1)—X(3)	5.91	6.77	5.04	3.49
LP X(4) → σ* P(1)—X(4)	0.64	–	–	–
LP X(4) → σ* P(1)—X(5)	5.91	6.76	5.04	3.49
LP X(5) → σ* P(1)—O(2)	37.27	4.57	3.48	2.23
LP X(5 → σ* P(1)—X(3)	5.90	6.77	5.04	3.49
LP X(5) → σ* P(1)—X(4)	5.91	6.76	5.04	3.49
LP X(5) → σ* P(1)—X(5)	0.64	–	–	–
σ P(1)—X(3) → σ*P(1)—O(2)	90.30	7.81	8.94	9.73
σ P(1)—X(4) → σ* P(1)—O(2)	90.29	7.81	8.94	9.73
σ P(1)—X(5) → σ* P(1)—O(2)	90.27	7.81	8.94	9.73

[a] See Fig. 1 for atoms numbering scheme.
[b] $E(2)$ means energy of hyper-conjugative interactions.

perturbation interaction energy $E(2)$. This energy represents the estimate of the off-diagonal NBO Fock matrix element. The stabilization energy $E(2)$ associated with i (donor) → j (acceptor) delocalization is estimated from the second-order perturbation approach as given below:

$$E(2) = \Delta E_{ij} = q_i \frac{F^2(i,j)}{\varepsilon_j - \varepsilon_i} \quad (1)$$

where q_i is the donor orbital occupancy, ε_i and ε_j are diagonal elements (orbital energies) and $F(i,j)$ is the off-diagonal Fock matrix element.

Table 2 shows the most relevant hyper-conjugative interactions calculated at B3LYP/LanL2DZ level for POX_3 compounds (X = F, Cl, Br and I). According to NBO analysis, the hyper-conjugative interactions are more favored in POF_3. A decrease in the hyper-conjugative interactions was observed along the series indicating that POI_3 compound is less stable than the other compounds. As can be seen in Table 2, the hyper-conjugative effect LP X → σ* P(1)—O(2) is more pronounced in POF_3 indicating that this interaction is very important for the stabilization of its structure. The interaction σ P(1)—X → σ* P(1)—O(2) is very high compared with the interactions for the other compounds, indicating that this effect

Table 3
Calculated atomic charges of the series of compounds POX_3 (X = F, Cl, Br, I) by natural bond orbital (NBO) analysis.

Atoms[a]	Atomic charges[b]			
	POF_3	$POCl_3$	$POBr_3$	POI_3
P(1)	2.47805	1.35990	1.06008	0.79047
O(2)	−0.91055	−0.80868	−0.79821	−0.79823
X(3)	−0.52249	−0.18374	−0.08729	0.00258
X(4)	−0.52250	−0.18374	−0.08729	0.00259
X(5)	−0.52251	−0.18375	−0.08729	0.00259

[a] See Fig. 1 for atoms numbering.
[b] Calculated at B3LYP/LanL2DZ level of theory.

Table 4
HOMO and LUMO energies, HOMO–LUMO energy gap and global reactivity descriptors data for POX_3 molecules (X = F, Cl, Br, I) calculated at B3LYP/LanL2DZ level of theory.

Molecular properties	POF_3	$POCl_3$	$POBr_3$	POI_3
E_{HOMO} (eV)	−10.510	−9.444	−8.779	−7.934
E_{LUMO} (eV)	−1.287	−3.087	−3.894	−4.816
$\Delta E_{HOMO-LUMO}$ (eV)	9.226	6.356	4.885	3.123
Ionization potential, *IP* (eV)	10.510	9.444	8.779	7.934
Electron affinity, *EA* (eV)	1.287	3.087	3.894	4.816
Electronegativity, χ (eV)	5.901	6.266	6.336	6.377
Chemical potential, μ (eV)	−5.901	−6.266	−6.336	−6.377
Chemical hardness, η (eV)	4.613	3.178	2.443	1.561
Chemical softness, s (eV^{-1})	0.108	0.157	0.205	0.320
Global electrophilicity index, ω (eV)	3.774	6.176	8.218	13.020

is very important for the stabilization of the molecule. According to the values reported in Table 2, the hyper-conjugative effects LP O(2) → σ* P(1)—X are responsible of the stabilization of POX_3 compounds (X = Cl, Br and I), moreover this interaction is of less importance for POF_3.

The atomic charges for the series of compounds POX_3 (X = F, Cl, Br and I) calculated by NBO method at B3LYP/LanL2DZ level of theory are presented in Table 3. According to Table 3, the P atoms have positive charges, the O(2) atoms have negative values and the halogen atoms have negative values except the iodine atoms. Considering the P(1) atoms, the maximum value of positive charge was observed for POF_3 molecule indicating that this atom could be a good acceptor. The O(2) atom for POF_3 has the maximum negative charge since O(2) in this molecule is a donor atom.

HOMO–LUMO analysis

The highest occupied molecular orbital (HOMO) and the lowest un-occupied molecular orbital (LUMO) are very important parameters for quantum chemistry. These values help to exemplify the chemical reactivity and kinetic stability of the molecule. The HOMO represents the ability to donate an electron and the LUMO as electron acceptor represents the ability to obtain an electron. In order to evaluate the energetic behavior of the title compounds, the HOMO–LUMO energy calculations were carried out by means B3LYP method using LanL2DZ basis sets. The energies and the pictorial illustration of HOMO and LUMO frontier molecular orbitals for all the compounds of the series are shown in Fig. 2. The positive and negative phase is represented in red and green color, respectively. The plots reveal that the HOMO for POF_3 and $POCl_3$ is primarily composed of fluorine and chlorine atoms and P(1) and O(2) while the HOMO for $POBr_3$ and POI_3 is located in the halogen atoms. The LUMO molecular orbital for the four molecules is spread over the entire molecule. The energy of the HOMO is directly related to the ionization potential, LUMO energy is directly related to the electron affinity and the difference of energy between both molecular orbitals is called as energy gap (E_{HOMO}–E_{LUMO}) that is an important parameter to evaluate the molecular chemical stability. In fact, a large HOMO–LUMO gap implies high molecular stability in the sense of its lower reactivity in chemical reactions. The energy value of HOMO and LUMO frontier molecular orbitals with the corresponding HOMO–LUMO energy gap for all compounds of the series are shown in Fig. 2 and listed in Table 4. By using HOMO and LUMO energy values for all the compounds of the series, the electronegativity (χ), chemical potential (μ), chemical hardness (η), softness (s) and global electrophilicity index (ω) can be calculated by using the following equations [37]:

$$\chi = \frac{(I+A)}{2} \text{ (Electronegativity)} \quad (2)$$

$$\mu = -\chi \text{ (Chemical potential)} \quad (3)$$

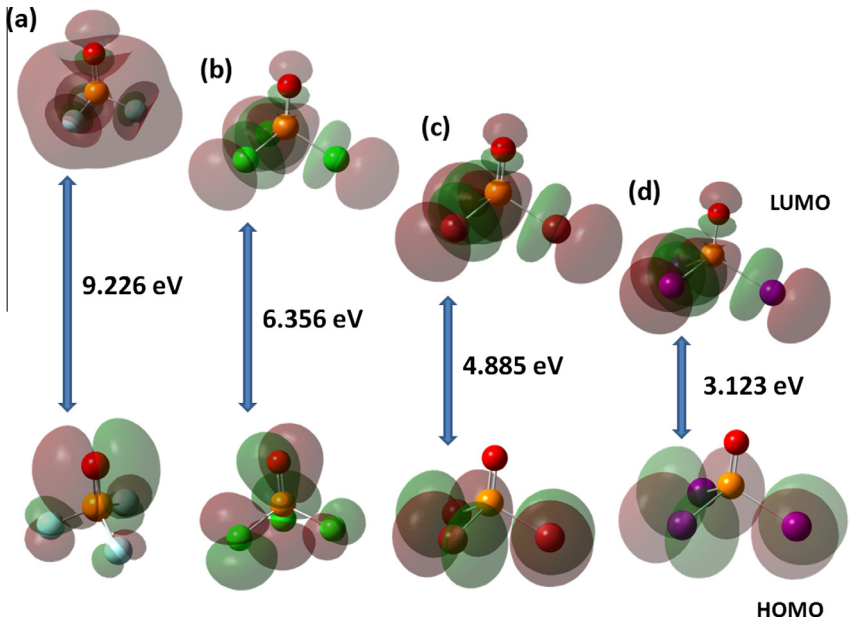

Fig. 2. Frontier molecular orbitals and HOMO–LUMO band gap for: (a) POF_3, (b) $POCl_3$, (c) $POBr_3$, (d) POI_3.

$$\eta = \frac{(I - A)}{2} \text{ (Chemical hardness)} \quad (4)$$

$$s = \frac{1}{2\eta} \text{ (Softness)} \quad (5)$$

$$\omega = \frac{\mu^2}{2\eta} \text{ (Global electrophilicity index)} \quad (6)$$

where I and A are ionization potential and electron affinity, respectively. According to the energies of HOMO and LUMO molecular orbitals, $I = -E_{HOMO}$ and $A = -E_{LUMO}$. The values of HOMO and LUMO energies, $\Delta E_{HOMO-LUMO}$, electronegativity, chemical potential, chemical hardness, softness and global electrophilicity index for all the molecules of the series are shown in Table 4. According to the values reported in Table 4, the $\Delta E_{HOMO-LUMO}$ for POF_3 is higher than other compounds indicating that this molecule is more stable and presents low reactivity. For POI_3, the energy gap is 3.123 eV. This value indicates that the compound presents low stability and is more reactive. This is in agreement with the results obtained in the synthesis of POI_3 that is very sensible to atmospheric conditions. Considering the chemical hardness, large HOMO–LUMO gap means a hard molecule and small HOMO–LUMO gap means a soft molecule. One can also relate the molecular stability to hardness, which means that the molecule with least HOMO–LUMO gap is more reactive. The usefulness of the global electrophilicity index has been recently demonstrated in understanding the toxicity of various pollutants in terms of their reactivity and site selectivity [38].

Vibrational analysis

The examined molecules belong to the C_{3v} molecular point group. They are characterized by 9 normal modes of vibration spanning the irreducible representations as $3A_1 + 3E$, all of them infrared and Raman active. For POF_3, $POCl_3$ and $POBr_3$ an analytical comparison was made of the theoretical geometries and wavenumbers with the available experimental values through root mean square deviations (RMSD). The best methods for describing the wavenumbers for POF_3 are MP2 and B3LYP with 6-31G(d) basis sets. For $POCl_3$, mPW1PW91 and MP2 methods with 6-311++G(d,p) basis sets reproduce better the experimental wavenumbers according to the RMSD values. For $POBr_3$ and POI_3 we found that the B3LYP/6-311++G(d,p) and MP2/6-311++G(d,p) combinations gave the best results in the description of the wavenumbers. The wavenumbers calculated at different levels of theory together with the experimental results for all the compounds of the series are listed in Tables S4–S7. Figs. 3 and 4 show the calculated IR and Raman spectra for all the compounds of the series and the experimental IR spectrum measured for POI_3 in solid state is shown in Fig. 5. According to the experimental IR spectrum, the P═O stretching vibration band appears at 1207 cm^{-1}. As the assignment of vibrational modes regarding the POI_3 molecule [12] was incomplete, we have decided to construct a semiempirical IR and Raman spectra obtained by using the experimental data combined with a scaling process applied to the remaining theoretical frequencies. A scale factor was obtained for each the remaining normal modes of vibration as the average ratio of the experimental and theoretical values of the POF_3, $POCl_3$ and $POBr_3$ molecules. As Raman activities we have used the theoretical ones. Force constants calculations were made at the B3LYP/6-31G(d) level of theory. The force constant matrices in Cartesian coordinates from the quantum chemical calculations were transformed into symmetry coordinates, defined as recommended by Pulay [36]. The defined coordinates appear in Table S8 (See Fig. S1). The resulting force constants were then scaled using the methodology described previously so as to reproduce the experimental wavenumbers. The final scale

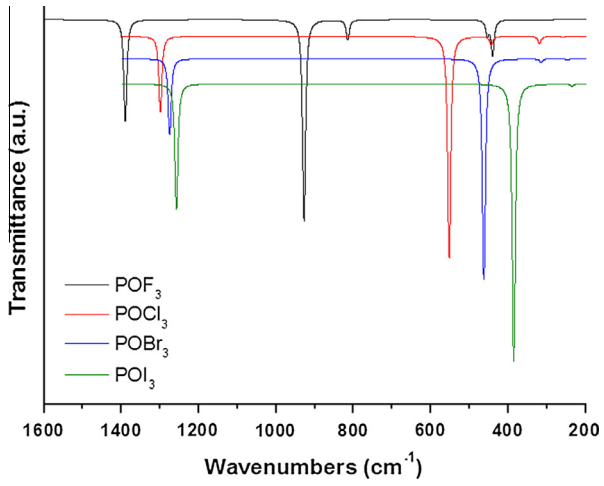

Fig. 3. IR spectrum for the series of compounds POX_3 (X = F, Cl, Br, I) calculated at B3LYP/6-311++G(d,p) level for F, Cl, Br and for the compound POI_3, the calculation was performed using B3LYP method using LanL2DZ basis sets for the iodine atoms and 6-311++G(d,p) for P and O.

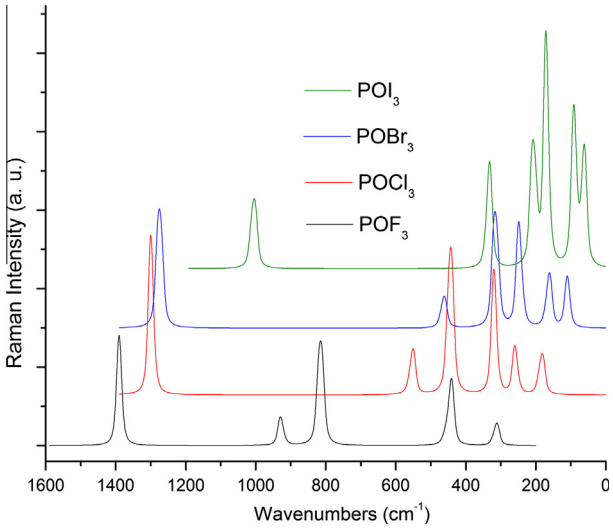

Fig. 4. Raman spectrum for the series of compounds POX_3 (X = F, Cl, Br, I) calculated at B3LYP/6-311++G(d,p) level for F, Cl, Br and for the compound POI_3, the calculation was performed using B3LYP method using LanL2DZ basis sets for the iodine atoms and 6-311++G(d,p) for P and O.

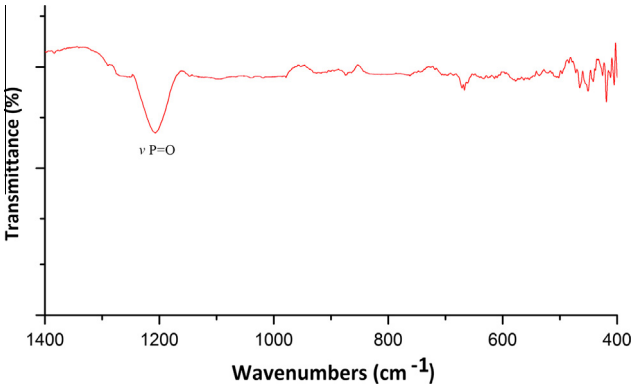

Fig. 5. Experimental IR spectrum of POI_3 measured in KBr pellets.

Table 5
Observed and calculated wavenumbers (cm^{-1}), infrared and Raman intensities, potential energy distribution (PED) and assignment for POF_3 compound.

Symmetry species	Mode	Observed[a]	Calculated[b]	Calc. SQM[c]	IR intensities[d]	Raman activities[e]	PED (>10%)	Assignment
A_1	1	1410.3	1405.1	1411.3	207.29	5.22	88 S_1 + 12 S_2	ν (P═O)
	2	873.9	845.8	873.9	34.75	11.38	88 S_2 + 11 S_1	ν_s (PF_3)
	3	482.1	455.0	482.7	30.83	1.25	95 S_3	δ_s (OPF_3)
E	4	989.9	986.5	989.3	207.91	1.01	97 S_4	ν_a (PF_3)
	5	471.3	444.6	470.6	40.51	2.34	50 S_5 + 22 S_6	ρ (OPF_3)
	6	329.0	310.2	329.6	0.19	0.86	84 S_6 + 53 S_5	δ_a (PF_3)
RMSD (cm^{-1})			21.5	0.65				

ν, Stretching; δ, deformation; ρ, rocking.
[a] Taken from Ref. [5].
[b] DFT B3LYP/6-31G(d).
[c] From scaled quantum mechanics force field.
[d] Units are km mol^{-1}.
[e] Raman activities in $Å^4$ $(amu)^{-1}$.

Table 6
Observed and calculated wavenumbers (cm^{-1}), infrared and Raman intensities, potential energy distribution (PED) and assignment for $POCl_3$ compound.

Symmetry species	Mode	Observed[a]	Calculated[b]	Calc. SQM[c]	IR intensities[d]	Raman activities[e]	PED (>10%)	Assignment
A_1	1	1296.0	1300.6	1296.5	137.91	12.65	98 S_1	ν (P═O)
	2	486.0	457.5	486.4	19.96	23.50	96 S_2	ν_s (PCl_3)
	3	267.0	261.9	267.0	2.75	7.77	91 S_3	δ_s ($OPCl_3$)
E	4	581.0	573.0	580.3	249.42	3.72	81 S_4 + 24 S_5	ν_a (PCl_3)
	5	337.0	321.2	337.0	8.34	7.73	58 S_5 + 22 S_4	ρ ($OPCl_3$)
	6	193.0	181.2	193.2	0.02	4.63	99 S_6 + 26 S_5	δ_a (PCl_3)
RMSD (cm^{-1})			14.9	0.40				

ν, Stretching; δ, deformation; ρ, rocking.
[a] From Ref. [6].
[b] DFT B3LYP/6-31G(d).
[c] From scaled quantum mechanics force field.
[d] Units are km mol^{-1}.
[e] Raman activities in $Å^4$ $(amu)^{-1}$.

Table 7
Observed and calculated wavenumbers (cm^{-1}), infrared and Raman intensities, potential energy distribution (PED) and assignment for $POBr_3$ compound.

Symmetry species	Mode	Observed[a]	Calculated[b]	Calc. SQM[c]	IR intensities[d]	Raman activities[e]	PED (>10%)	Assignment
A_1	1	1261.0	1279.9	1261.7	113.25	13.46	99 S_1	ν (P═O)
	2	340.0	332.6	335.9	6.44	17.64	78 S_2 + 32 S_3	ν_s (PBr_3)
	3	173.0	163.4	176.6	0.03	6.62	68 S_3 + 22 S_2	δ_s ($OPBr_3$)
E	4	488.0	486.1	492.1	194.64	1.80	57 S_4 + 42 S_5	ν_a (PBr_3)
	5	267.0	249.7	259.1	2.24	5.83	50 S_5 + 43 S_4	ρ ($OPBr_3$)
	6	118.0	106.3	117.5	0.01	2.89	100 S_6 + 16 S_5	δ_a (PBr_3)
RMSD (cm^{-1})			13.2	4.58				

ν, Stretching; δ, deformation; ρ, rocking.
[a] From Ref. [7].
[b] DFT B3LYP/6-31G(d).
[c] From scaled quantum mechanics force field.
[d] Units are km mol^{-1}.
[e] Raman activities in $Å^4$ $(amu)^{-1}$.

factors for the POX_3 (X = F, Cl, Br) molecules are shown in Table S9. The obtained potential energy distributions (PED), has confirmed all of the experimental assignments and are presented together with the resulting wavenumbers, final RMSD values and infrared and Raman activities in Tables 5–7. Finally, the scaled force matrices in symmetry coordinates were transformed into internal coordinates. The scaled internal force constants are listed in Table S10. A decrease of wavenumbers corresponding to the P═O stretching mode is observed along the series. This should correspond to an increase in the involved bond length which is reflected in the theoretical results. However, experimentally this is true only when we move from the fluorine to the chlorine compound. The P═O bond distance for $POBr_3$ is shorter than expected. Anyway, $POBr_3$ geometry was measured five decades ago, and should be re-measured using more accurate methods.

Regarding geometry results, an increase in the P═O bond length is observed along the series. This is in agreement with the experimental trend, except when we move from the chlorine to the bromine compound, where the P═O bond length is shorter than expected. This trend goes together with a decrease in energy of

the P—O bond, reflected in a lower frequency of vibration for the P═O stretching mode.

Conclusions

In this article we report the structural results obtained by quantum chemical calculations for the series of compounds with general formula POX_3 (X = F, Cl, Br, I). For the calculations we have used *ab initio* and DFT methods with different basis sets and we compare with the experimental results previously reported only for POF_3, $POCl_3$ and $POBr_3$. The compound POI_3 was synthesized by reaction with CH_3POI_2 as a precursor. The resultant product was only characterized by IR spectroscopy. According to the calculations, an increase in the P═O bond length is observed along the series because of the high atomic volume of the halogen atom produces a lengthening of the P═O bond length. This trend goes together with a decrease in energy of the P—O bond, reflected in a lower frequency of vibration for the P═O stretching mode as was observed in the vibrational analysis. According to NBO analysis, the hyper-conjugative interactions are more favored in POF_3. A decrease in the hyper-conjugative interactions was observed along the series indicating that POI_3 compound is less stable than the other compounds. The hyper-conjugative effect LP $X \rightarrow \sigma^*$ P(1)—O(2) is more pronounced in POF_3 indicating that this interaction is very important for the stabilization of its structure. HOMO–LUMO analysis reveals that the $\Delta E_{HOMO-LUMO}$ for POF_3 is higher than other compounds indicating that this molecule is more stable and presents low reactivity. For POI_3, the energy gap is 3.123 eV. This value indicates that the compound is the most reactive and has the lowest stability along the series. This is in agreement with the results obtained in the synthesis of POI_3 that is very sensible to atmospheric conditions.

Acknowledgments

J.E.G., D.M.G., H.E.L. and A.B.A. thank CIUNT and CONICET (PIP 0205) for financial support. J.E.G. and D.M.G. thank CONICET for fellowships.

Appendix A. Supplementary material

Supplementary data associated with this article can be found, in the online version, at http://dx.doi.org/10.1016/j.molstruc.2014.10.060.

References

[1] K. Nakamoto, Infrared and Raman Spectra of Inorganic and Coordination Compounds, Part A, fifth ed., Wiley-Interscience, New York, 1997.
[2] Y.S. Li, M.M. Chem, J.R. Durig, J. Molec, J. Molec. Struct. 14 (1972) 261.
[3] T. Moritani, K. Kuchitsu, Y. Morino, Inorg. Chem. 10 (1971) 344.
[4] I.H. Secrist, L.O. Brockway, J. Amer. Chem. Soc. 66 (1945) 1941.
[5] A.J. Downs, G.P. Gaskill, S.B. Saville, Inorg. Chem. 21 (1982) 3385.
[6] S.R. Gupta, A.V.R. Warrier, Spectrochim. Acta 39A (6) (1983) 529.
[7] H. Gerding, M. Van Driel, Rec. Trav. Chim. 61 (1942) 419.
[8] R.R. Filgueira, C.E. Blom, A. Müller, Spectrochim. Acta 36A (1980) 745.
[9] Sh.Sh. Nabiev, B.S. Khodzhiev, J. Inorg. Chem. 39 (1994) 1628.
[10] B.W. Moores, L. Andrews, J. Phys. Chem. (1989) 1902.
[11] H. Selig, H.H. Claasen, J. Chem. Phys. 44 (1966) 1404.
[12] A.W. Allaf, Spectrochim. Acta 54A (1998) 921.
[13] J.C. Sheldon, S.Y. Tyree, J. Am. Chem. Soc. 80 (1958) 4775.
[14] V.A. Shlyapochnikov, O.G. Strukov, S.S. Dubov, L.N. Shitov, J. Inorg. Chem. 14 (1969) 1536.
[15] R.J.H. Clark, D.M. Rippon, Mol. Phys. 28 (1974) 305.
[16] A. Muller, B. Krebs, A. Fadini, O. Glemser, S.J. Cyvin, J. Brunvoll, B.N. Cyvin, I. Elvebredd, G. Hagen, B. Vizi, Z. Naturforsch. 23A (1968) 1656.
[17] L. Doyennette, J. Chim. Phys. 58 (1961) 487.
[18] C. Socolsky, S.A. Brandán, A. Ben Altabef, E.L. Varetti, J. Mol. Struct. Theochem 672 (2004) 45.
[19] V.G. Kostina, N.G. Fescchenko, A.V. Kirsanov, Z. Obshchei Khimii 43 (1973) 207.
[20] N.G. Fescchenko, V.G. Kostina, A.V. Kirsanov, Z. Obshchei Khimii 43 (1972) 208.
[21] M.J. Frisch, J.A. Pople, J.S. Binkley, J. Chem. Phys. 80 (1984) 3265; M. J. Frisch, G. W. Trucks, H. B. Schlegel, G. E. Scuseria, M. A. Robb, J. R. Cheeseman, J. A. Montgomery Jr., T. Vreven, K. N. Kudin, J. C. Burant, J. M. Millam, S. S. Iyengar, J. Tomasi, V. Barone, B. Mennucci, M. Cossi, G. Scalmani, N. Rega, G. A. Petersson, H. Nakatsuji, M. Hada, M. Ehara, K. Toyota, R. Fukuda, J. Hasegawa, M. Ishida, T. Nakajima, Y. Honda, O. Kitao, H. Nakai, M. Klene, X. Li, J. E. Knox, H. P. Hratchian, J. B. Cross, C. Adamo, J. Jaramillo, R. Gomperts, R. E. Stratmann, O. Yazyev, A. J. Austin, R. Cammi, C. Pomelli, J. W. Ochterski, P. Y. Ayala, K. Morokuma, G. A. Voth, P. Salvador, J. J. Dannenberg, V. G. Zakrzewski, S. Dapprich, A. D. Daniels, M. C. Strain, O. Farkas, D. K. Malick, A. D. Rabuck, K. Raghavachari, J. B. Foresman, J. V. Ortiz, Q. Cui, A. G. Baboul, S. Clifford, J. Cioslowski, B. B. Stefanov, G. Liu, A. Liashenko, P. Piskorz, I. Komaromi, R. L. Martin, D. J. Fox, T. Keith, M. A. Al-Laham, C. Y. Peng, A. Nanayakkara, M. Challacombe, P. M. W. Gill, B. Johnson, W. Chen, M. W. Wong, C. González, J. A. Pople, Gaussian 03, revision C.02; Gaussian Inc: Wallingford, CT, 2004.
[22] C. Møller, M.S. Plesset, Phys. Rev. 46 (1934) 618.
[23] R. Krishnan, J.S. Binkley, R. Seeger, J.A. Pople, J. Chem. Phys. 72 (1980) 650.
[24] A.D. McLean, G.S. Chandler, J. Chem. Phys. 72 (1980) 5639.
[25] M.J. Frisch, J.A. Pople, J.S. Binkley, J. Chem. Phys. 80 (1984) 3265.
[26] W.J. Hehre, P.V.R. Schleyer, J.A. Pople, Ab initio Molecular Orbital Theory, Wiley, New York, 1986.
[27] A.D. Becke, J. Chem. Phys. 98 (1993) 5648.
[28] C. Lee, W. Yang, R.G. Parr, Phys. Rev. B 37 (1988) 785.
[29] C. Alamo, B. Barone, J. Chem. Phys. 108 (1998) 664.
[30] D.M. Gil, O.E. Piro, G.A. Echeverría, M.E. Tuttolomondo, A. Ben Altabef, Spectrochim. Acta A 116 (2013) 122.
[31] D.M. Gil, M.E. Tuttolomondo, A. Ben Altabef, Spectrochim. Acta A 123 (2014) 290.
[32] M.E. Defonsi Lestard, M.E. Tuttolomondo, D.A. Wann, H.E. Robertson, D.W.H. Rankin, A. Ben Altabef, J. Chem. Phys. 131 (2009) 214303.
[33] M.J. Frisch, A.B. Nielsm, A.J. Holder, Gaussview User Manual, Gaussian, Pittsburgh, 2008.
[34] E.D. Glendening, J.K. Badenhoop, A.D. Reed, J.E. Carpenter, F.F. Weinhold, Theoretical Chemistry Institute, University of Wisconsin, Madison, WI, 1996.
[35] W.B. Collier, Program FCARTP (QCPE # 631), Department of Chemistry, Oral Roberts University, Tulsa, OK, 1992.
[36] P. Pulay, G. Fogarasi, G. Pongor, J.E. Boggs, A. Vargha, J. Am. Chem. Soc. 105 (1983) 7037.
[37] R. John Xavier, P. Dinesh, Spectrochim. Acta A 113 (2013) 171.
[38] J. Parthasarathi, J. Padmanabhan, U. Sarkar, B. Maiti, V. Subramanian, P.K. Chattaraj, Internet Electron. J. Mol. Des. 2 (2003) 798.